Probing Sources of Decoherence at Defects and Interfaces in Superconducting Quantum Materials and Devices

Akshay A. Murthy[1,*], Roberto dos Reis[2,3,4], Stephanie M. Ribet[2,3], Mattia Checchin[1], Anna Grassellino[1], Vinayak P. Dravid[2,3,4], and Alexander Romanenko[1,5]

[1.] Superconducting Quantum Materials and Systems Division, Fermi National Accelerator Laboratory, Batavia, Illinois, USA
[2.] Department of Materials Science and Engineering, Northwestern University, Evanston, IL USA
[3.] International Institute of Nanotechnology, Northwestern University, Evanston, IL USA
[4.] NU*ANCE* Center, Northwestern University, Evanston, IL USA
[5.] Applied Physics and Superconducting Technology Division, Fermi National Accelerator Laboratory, Batavia, Illinois, USA
* Corresponding author: amurthy@fnal.gov

Superconducting qubits have emerged as a platform technology for potentially addressing computational problems deemed intractable with classical computing. Despite recent advances enabling multiqubit designs that exhibit coherence lifetimes on the order of hundreds of µs, defects and amorphous oxides continue to curb device performance by dissipating electromagnetic energy. As such, extending this technology to large-scale devices with the requisite reliability and performance metrics necessitates an increased understanding and control over imperfections and impurities [1,2,3]. Experimental and theoretical investigations have led researchers to understand quantum decoherence is dictated by deviations from crystalline order on the nanoscale. Thus, the high-resolution nature of electron microscopy makes it an indispensable tool for identification of decoherence sources.

Through a combination of scanning transmission electron imaging and diffraction methods, we interrogate the thin metal films integral for superconducting qubit operation and observe structural and chemical features that can potentially serve as decoherence sources. This includes the presence of localized strain at grain boundaries and metal/substrate interfaces (Figure 1). Such localized strain can induce changes in the superconducting critical temperature and superconducting order parameter. Additionally, through *in situ* cooling experiments, we map the distribution of resistive hydride precipitates at cryogenic temperatures. These precipitates exhibit smaller superconducting gaps than the surrounding regions. Both aspects can potentially introduce decoherence in these quantum devices.

Further, by employing the fluctuation electron microscopy (FEM) technique, we are able to better understand the medium range order (MRO) present in the amorphous oxides that inevitably form in these systems. Specifically, this involves radial fitting amorphous rings to each diffraction pattern using least squares regression model followed by calculating the radial intensity and normalized variance of the annular means as a function of scattering angle [4]. Through this analysis we observe a variation in bond distances in the surface oxide (Figure 2). Such variation can lead to low frequency noise, which helps explain previous experimental data highlighting the lossy nature of this oxide. Equipped with these findings, we seek to intelligently fabricate superconducting qubits and extend coherence times [5].
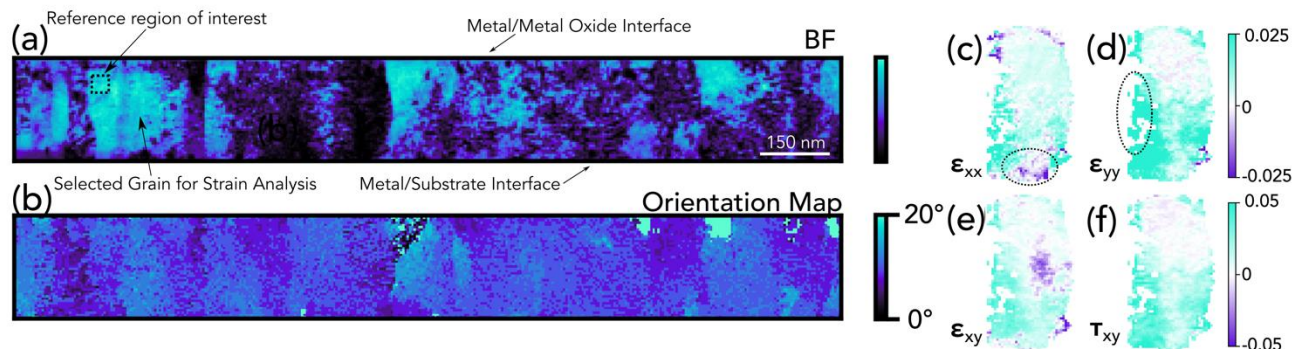
Figure 1. Nb film structure (a) Bright field and (b) Relative in-plane orientation map of Nb grains. Relative strain maps of an on-axis Nb grain are provided (c) along the substrate axis (ε_{xx}) and (d) along the film growth axis (ε_{yy}). Regions of compressive strain at the metal/substrate interface and tensile strain near the grain boundary are circled. Shear strain in the sample plane (ε_{xy}) along with rotational strain in the sample plane (τ_{xy}) are provided in (e) and (f) respectively. The selected grain and unstrained reference regions are indicated as well.
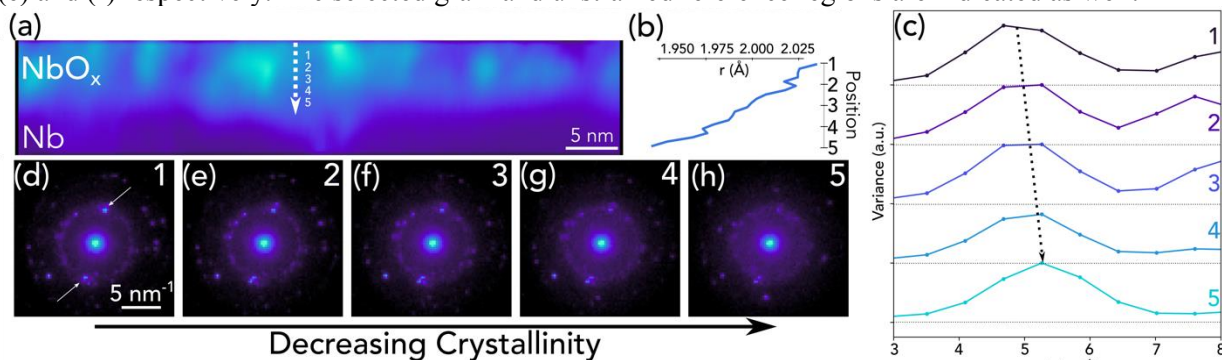
Figure 2. Nb/O interface (a) DF image of Nb oxide/Nb constructed using a virtual detector that matched the diffraction ring of Nb oxide. (b) Variation in bond distance as a function of regions labeled 1-5 in the DF image. (c) Annular mean of normalized variances as a function of position. The peak positions are observed to red-shift from region 1 to region 5. The reciprocal of the peak positions in these plots were used to calculate the respective bond distances at each region. (d-h) Diffraction patterns taken from regions 1, 2, 3, 4, and 5, respectively. As the distinct diffraction spots indicated by the arrows fade in intensity from region 1 to region 5, it is apparent that the Nb oxide decreases in crystallinity in the direction away from the surface.

References:

[1] A A Murthy *et al*, arXiv, (2022), 2203.08710
[2] S M Ribet*, A A Murthy* *et al,* Materials Today, **50** (2021)*,* pp. 100-115
[3] A A Murthy *et al*, Applied Physics Letters, **120** (2022), 044002
[4] E Kennedy *et al*, Applied Physics Letters, **117** (2020), 091903